Quasi-Z-source-based bidirectional DC-DC converters for renewable energy applications

Journal title;
International Transactions on Electrical Energy Systems

First published: **01 Apr 2021**

Received <day> <Month>, <year>; | Revised <day> <Month>, <year>; | Accepted <day> <Month>, <year>

DOI: xxx/xxxx

ARTICLE TYPE

Quasi-Z-Source-based Bidirectional DC-DC Converters for Renewable Energy Applications†

Yuba Raj Kafle*[1] | M.J. Hossain[2] | Muhammad Kashif[3]

[1]School of IT and Engineering, Melbourne Institute of Technology, NSW, Australia
[2]School of Electrical and Data Engineering, University of Technology Sydney, NSW, Australia
[3]School of Engineering, Macquarie University, NSW, Australia

Correspondence
*Yuba Raj Kafle, School of IT and Engineering, Melbourne Institute of Technology, 154-158 Sussex St, Sydney NSW 2000. Email: ykafle@academic.mit.edu.au

Present Address
School of IT and Engineering, Melbourne Institute of Technology, 154-158 Sussex St, Sydney NSW 2000.

Abstract

This paper presents a design, analysis and implementation of a novel impedance-source-based bidirectional DC-DC converter. The proposed converter employs an impedance network to the existing dual-active-bridge (DAB) circuit. It inherits all the advantages of the DAB converter along with extra benefits.Compared with the traditional isolated dc-dc converter, the proposed converter improved the boost ability of the converter. Also, the converter can withstand the shoot-through phenomenon in an H-bridge, improving the reliability.The converter can work in the normal buck-/boost DAB mode when extra boost is not required. The bidirectional feature is inherent along with soft switching capability. It is therefore well-suited for the applications, where wide range of voltage gains are required such as renewable energy systems. The topological configuration and control strategy of the proposed topology in both operational modes are discussed. Simulation and experiments have been carried out to demonstrate the effectiveness of the proposed converter topology. The peak efficiency 97% was observed at the rated load of 500 W.

KEYWORDS:
Impedance-source converter, DC-DC Converter, bidirectional, Dual active bridge

1 | INTRODUCTION

Renewable-energy penetrations are increasing in recent years due to the growing interest in clean energy alternatives rather than traditional generation. This growing number of renewable integrations leads to an increasing number of storage systems to solve the issue of the intermittent nature of these renewable sources. A bidirectional DC-DC converter is essential for such system to transfer power between two DC buses [1,2,3,4]. Figure 1 shows the typical system configuration of distributed power generation where a bidirectional dc-dc converter is needed for battery charging systems and power transfer between two DC buses. Multiple DC-DC converters are connected to common DC-bus which can connect to different load and sources. Another application area of bidirectional DC-DC converters is electric vehicles [5 6 7], motor drive applications [8], uninterruptible power supplies (UPS) [9,10], solid-state transformers [11], and more. Bidirectional DC-DC converters are divided into two types: non-isolated and isolated types. A non-isolated bidirectional DC-DC converter is suitable where galvanic isolation is not required, making the converter compact and efficient [12,13,14]. An isolated bidirectional DC-DC converter is needed to provide electrical isolation between input and output for protecting equipment and operators [15].

†This is an example for title footnote.
[0]**Abbreviations:** ANA, anti-nuclear antibodies; APC, antigen-presenting cells; IRF, interferon regulatory factor

The most typical configuration of a bidirectional DC-DC converter is the DAB converter consisting of two single-phase H-bridge topologies interfaced by a high-frequency transformer[16]. Each bridge is controlled with a 50% constant duty cycle to generate a high-frequency square-wave voltage at its transformer terminals. The power flow from each bridge is controlled by a phase shift between the two bridges[17,18,19,20]. Power is delivered from one bridge to the other, which generates square-wave pulses with a leading phase angle. The output voltage depends on three parameters: the transformer turns ratio, the switching frequency and the transformer's leakage inductance. These parameters are usually fixed for the designed converter prototype, hence it has limited voltage-regulation ability and a lack of flexibility[21]. This paper aims to reduce the drawback of the DAB, thereby improving both the voltage regulation range and the reliability of the converter.

The impedance-source-based (ZS) converter is a new way of power delivery applicable for renewable-energy systems, originally proposed by Fang Z. Peng[22,23]. These converters overcome many limitations of traditional voltage-source and current-source power converters, and the concept of an ZS network can be applied to DC-DC, DC-AC, AC-AC and AC-DC power conversions. Hence there is an increasing research interest in impedance-source-based converters[24]. In[25,26,27] a high gain impedance source based dc-dc converter suitable for renewable energy applications were proposed.Many extensions of ZS converters with additional benefits have been reported in the literature such as for the quasi-z-source (qZS) as reported in[28].A qZS based high step-up DC-DC converter has been presented in[29] for improved voltage gain. In[30] a qZS based bidirectional dc-dc converter with symmetric structure is presented, however the active and passive component count is high increasing the cost. The qZS features low inrush current, lower component count, high control flexibility, and continuous dc input current[31,32].

This paper proposes a bidirectional quasi-Z-source based dc-dc converter where a bidirectional qZS network is added at the input side of the DAB converter (abbreviated as qDAB). Due to a high frequency transformer, the converter has an advantage of reduced power density and ground leakage current is minimum.This converter has two degree of freedom to boost the input voltage either by transformer turns ratio or by the utilization of extra switching state- the shoot-through state (simultaneous conduction of both switches of the same phase leg of the converter) in its operation states, so the converter boost ability gets improved.Thus the proposed converter is suitable for distributed power generation systems. Apart from that, the converter can also be used for EV charger, solid-state transformer, fuel cell application for distributed generation etc. Compared with the traditional bidirectional isolated dc-dc converter, this converter has higher boost ability, low input current ripple, wider voltage regulation range, simple control and high reliability. The circuit structure of the qDAB is shown in Fig. 2 , consisting of impedance network, and a high-frequency transformer connecting two H-bridges on either side.

The remainder of this paper is structured as follows: Section 2 gives an overview of the proposed topology, the control methods of the converter are presented in Section 3, Section 4 illustrates the comparison of proposed converter with other topologies, Section 5 provides simulation and experimental results. Section 6 concludes the paper.

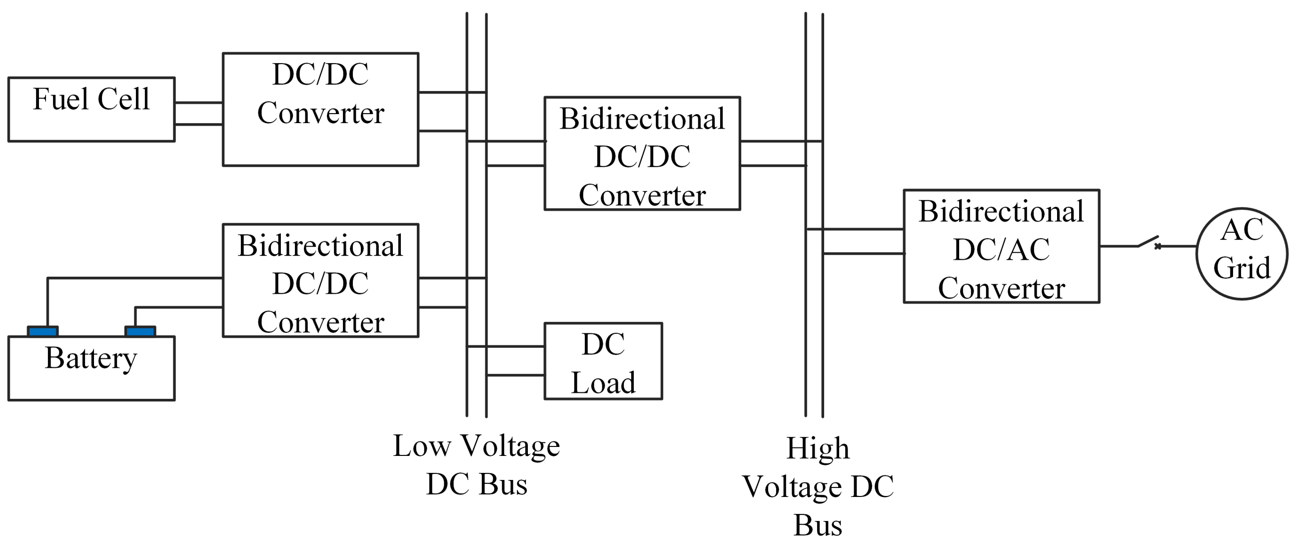

FIGURE 1 A typical distributed power generation system

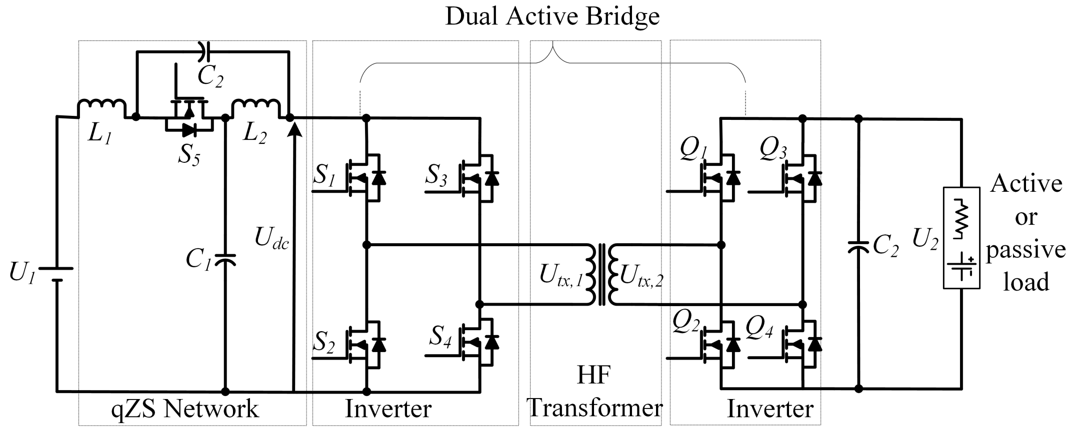

FIGURE 2 Proposed converter topology

2 | DESCRIPTION OF PROPOSED QDAB)

Fig. 2 shows the proposed converter topology, consisting of an impedance network (L_1, L_2, C_1, C_2 and S_5), and a high-frequency transformer connecting the two H-bridges, one on either side. The diode in the qZS network is replaced by an active switch with a parallel diode to make the converter bidirectional. The impedance network provides extra boost ability utilizing an additional switching state called a "shoot-through" state. In a shoot-through state, any leg or all legs of the H-bridge inverter is short-circuited.

Power flow from left to right is considered as a forward power flow and from right to left is called reverse power flow. In the forward-power-transfer mode, the converter has the flexibility to work in a boost mode of operation if extra boost is required utilizing shoot-through states. In reverse-power-transfer mode, the converter can work as a conventional DAB converter performing a buck/boost operation.

In the forward-power-transfer mode, the converter goes through three operational states: active state, zero state and shoot-through state.

2.1 | Active State

During the active state, cross-connected switch pairs (S_1 and S_4 or S_2 and S_3) conduct and the power is transferred from the input side to the output side through an isolation transformer as shown in Fig. 3 . The voltage across the primary of the transformer is the dc-link voltage $\pm V_{dc}$ which is reflected to the secondary side. The dc source charges the quasi-Z source network capacitors, while the inductor transfers its energy to the load.

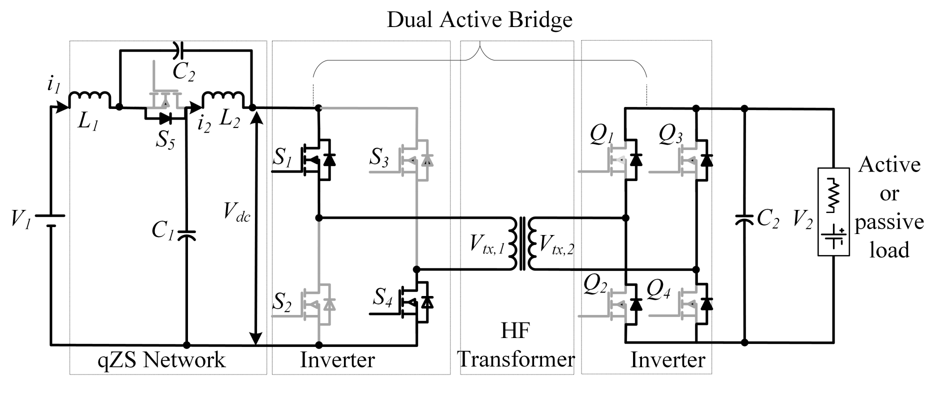

FIGURE 3 Active State

2.2 | Zero State

During the zero state, the primary winding of the isolation transformer is shorted through either the top (S_1 and S_3) or bottom (S_2 and S_4) switches, thus the primary current freewheels either from upper or lower switches. So, no power is transferred from primary to secondary side. The circuit state during this operation mode is shown in Fig.4 .

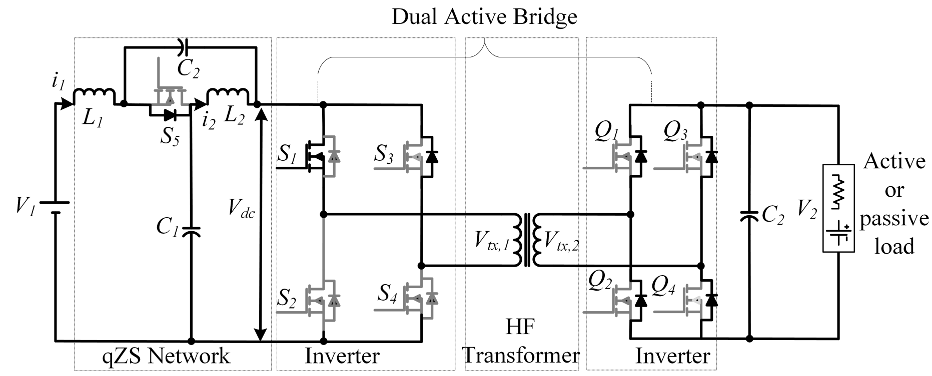

FIGURE 4 Zero State

2.3 | Shoot-through State

As stated previously, the shoot-through state is when one or all legs in the H-bridge inverter is turned on. This state boosts the dc-link voltage and also protects the circuit from damage, thus improving the system's reliability significantly. The circuit structure during this operation mode is shown in Fig. 5 where all four switches (S_1 -S_4) are conducting, leading the transformer voltage ($V_{tx,1}$) to drop to zero. During this state, the diode D_5 will be reverse biased and the capacitor voltage C_1 and C_2 charges the inductors L_1 and L_2 without shorting the DC capacitors.

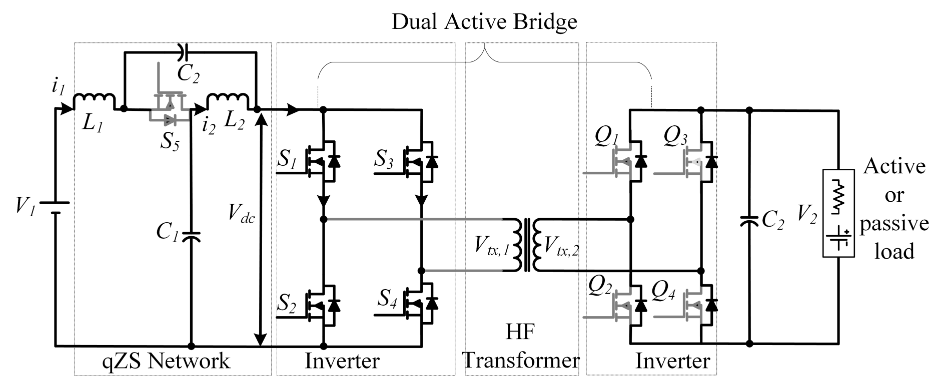

FIGURE 5 Shoot-through State

Assume that T_S is the switching time period, T_{ST} is the shoot-through switching time and T_{NST} is the non-shoot through (active and zero state) time period. The shoot-through duty cycle is thus $D_{ST} = T_{ST}/T_S$. During the non-shoot-through state T_{NST} (Figs. 3 and 4) the following equations holds:

$$v_{L1} = V_1 - V_{C1},\ v_{L2} = -V_{C2},\ I_{C1} = I_{L1} - I_l,\ I_{C2} = I_{L2} - I_l \tag{1}$$

During the shoot-through interval T_{ST} (Fig. 5) the following equations can be obtained

$$v_{L1} = V_1 + V_{C2},\ v_{L2} = V_{C1},\ I_{C1} = -I_{L2},\ I_{C2} = -I_{L1} \tag{2}$$

During the steady state, the average voltage across the inductor over a cycle is zero. From (1) and (2), we have

$$\begin{cases} V_{L1} = \bar{v}_{L1} = \frac{T_{ST}\ (V_1+V_{C2})+T_{NST}(V_1-V_{C1})}{T_S} = 0 \\ V_{L2} = \bar{v}_{L2} = \frac{T_{ST}\ (V_{C1})+T_{NST}(-V_{C2})}{T_S} = 0 \end{cases} \tag{3}$$

The capacitor voltages and DC-link voltage thus can be obtained as:

$$V_{C1} = \frac{1 - D_{ST}}{1 - 2D_{ST}} V_1,\ V_{C2} = \frac{D_{ST}}{1 - 2D_{ST}} V_1 \tag{4}$$

$$V_{dc} = V_{C1} + V_{C2} = \frac{1}{1 - 2D_{ST}} V_1 = BV_1 \tag{5}$$

where B is the boost factor of the converter. From (5), it is clear that the converter boost ability can be increased by increasing the shoot-through duty cycle. The output voltage of the converter can be obtained as:

$$V_2 = \frac{n}{1 - 2D_{ST}} V_1 = BnV_1 \tag{6}$$

where n is the transformer turns ratio.

During the reverse-power-transfer mode, the converter can work as a normal DAB converter. The switch S_5 is turned on, shorting the diode which allows the backward power flow. The passive impedance network (L_1, L_2, C_1 and C_2) acts as a low-pass LCL filter network. The power flow is controlled by modulation of the switches Q_1-Q_4 and S_1 S_4. The circuit structure during the reverse-power-transfer mode is shown in Fig. 6 .

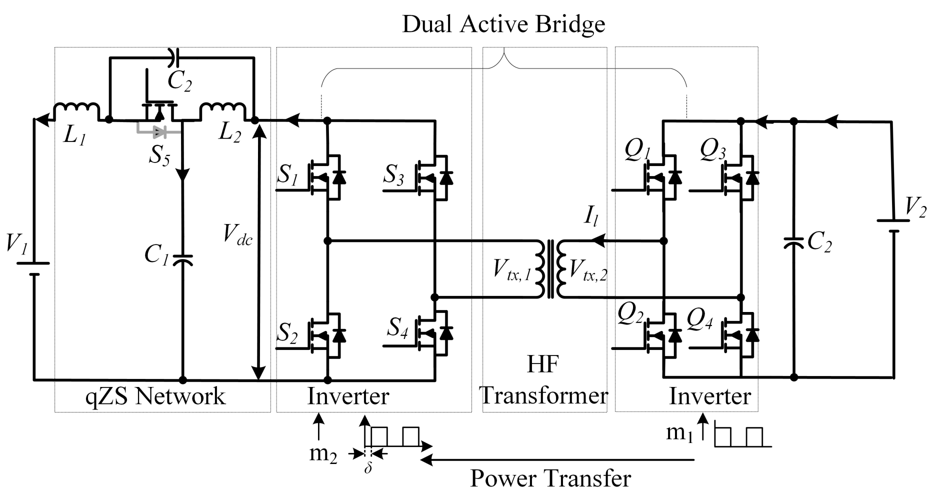

FIGURE 6 Reverse-power-transfer mode

2.4 | Design Parameters

In this section, an overview of the design process of the proposed DC-DC converter is discussed. The design parameters of passive components of qZS network (L_1, L_2, C_1 and C_2) are introduced. The inductors and capacitors of qZS network is selected based on the desired ripple current and ripple voltage during the active states and shoot-through states.

TABLE 1 The voltage stress across the switch and capacitor

Voltage stress on switching device	Voltage stress on capacitor
$V_{sw} = \frac{1}{1-2D_{ST}} V_1$	$V_{C1} = \frac{1-D_{ST}}{1-2D_{ST}} V_1$, $V_{C2} = \frac{D_{ST}}{1-2D_{ST}} V_1$

Substituting V_{c2} from (4) into (2), the V_{L1} can be given by:

$$V_{L1} = \frac{1 - D_{ST}}{1 - 2D_{ST}} V_1 \tag{7}$$

During shoot-through state, the inductor current increases linearly. The inductor current ripple (ΔI_{L1}) in the L_1 can be derived as:

$$\Delta I_{L1} = \frac{V_{L1}\Delta T}{L_1} = \frac{(1 - D_{ST})D_{ST}T_S}{L_1(1 - 2D_{ST})} V_1 \tag{8}$$

where ΔT is the time interval during shoot-through operation, $D_{ST}T_S$. Similarly, the current ripple (ΔI_{L2}) through the inductor L_2 is derived as:

$$\Delta I_{L2} = \frac{V_{L2}\Delta T}{L_2} = \frac{(1 - D_{ST})D_{ST}T_S}{L_2(1 - 2D_{ST})} V_1 \tag{9}$$

Thus the required value of inductor is designed using (8) and (9) choosing the acceptable current ripple. Similarly, the qZS capacitors can be designed to limit the DC-link voltage ripple. From capacitors currents (I_{C1} and I_{C2}) from (1), the capacitor voltage ripples (ΔV_{C1}, ΔV_{C2}) on capacitors (C_1 and C_2) can be derived as

$$\Delta V_{C1} = \frac{I_{L2}\Delta T}{C_1} = \frac{I_{L2}D_{ST}T_S}{C_1} \tag{10}$$

$$\Delta V_{C2} = \frac{I_{L1}\Delta T}{C_2} = \frac{I_{L1}D_{ST}T_S}{C_2} \tag{11}$$

The value of capacitance is calculated using (10) and (11) taking into account an acceptable voltage ripple on them.

2.5 | Voltage Stress Analysis

This section presents the voltage stress of the proposed converter across switches and capacitors. The voltage stress are important factors that affect the performance of the converter and the size of converter cost and volume. The proposed converter achieves lower voltage stresses on the power switches and capacitors as shown in Table1 . The voltage across the capacitors C_1 and C_2 is lower reducing the required capacitor rating. Similarly, the input current is continuous due to input inductor L_1, which greatly reduces the input stress. The switching stress across the switch is $B*V_1$.

3 | CONTROL METHOD OF QDAB

During the forward-power-transfer mode, PWM shoot-through method is used whereas, during the reverse-power-transfer mode, the phase shift modulation technique is used in the qDAB. Details of the control technique for both operation modes are given below.

3.1 | Forward Power Flow Control

In this operational mode, the switches of the input-side bridge (S_1 -S_4) are switched on and the switches at the output-side bridge (Q_1-Q_4) act as a synchronous rectifier. The boost ability can be obtained not only by the transformer turns ratio but also by the introduction of shoot-through states. A PWM shoot-through control technique is used which is derived from PWM control with a shifted shoot-through modulation technique. In this modulation technique, shoot-through states are generated within zero states which are equally distributed during the switching intervals as shown in Fig. 7 . During this switching cycle, the converter goes into six states (within t_0 - t_6) over a cycle with two active states ($t_0 < t < t_1$) and ($t_3 < t < t_4$), two zero states ($t_1 < t < t_2$ and $t_4 < t < t_5$) and two shoot-through state ($t_2 < t < t_3$ and $t_5 < t < t_6$). The active state is kept intact and is independently controllable. Only two shoot-through states are used per period, which minimizes the switching loss. In the switching cycle, switches S_1 and S_2 are operated at the switching frequency f_s while switches S_3 and S_4 operate at twice the switching frequency $2*f_s$. Also, the position of shoot-through state is within a zero state and is independent of the active state which is independently controllable, allowing a full range of voltage regulation.

Fig. 8 shows the logic used to generate the modulation technique. A single saw-tooth carrier signal is used to generate the PWM signals and the shoot-through signals by comparing with reference signals. The modulation logic is simple and is easily implantable in an analog or digital controller such as a digital signal processor (DSP), Field-programmable gate array (FPGA), dSPACE, a microcontroller, logic gates etc. The control switching logic is implemented in a digital controller (a Xilinx Spartan 6 FPGA) using the MATLAB Simulink HDL coder toolbox. The gate signal, with a 10% shoot-through duty cycle, is shown in Fig. 9 .

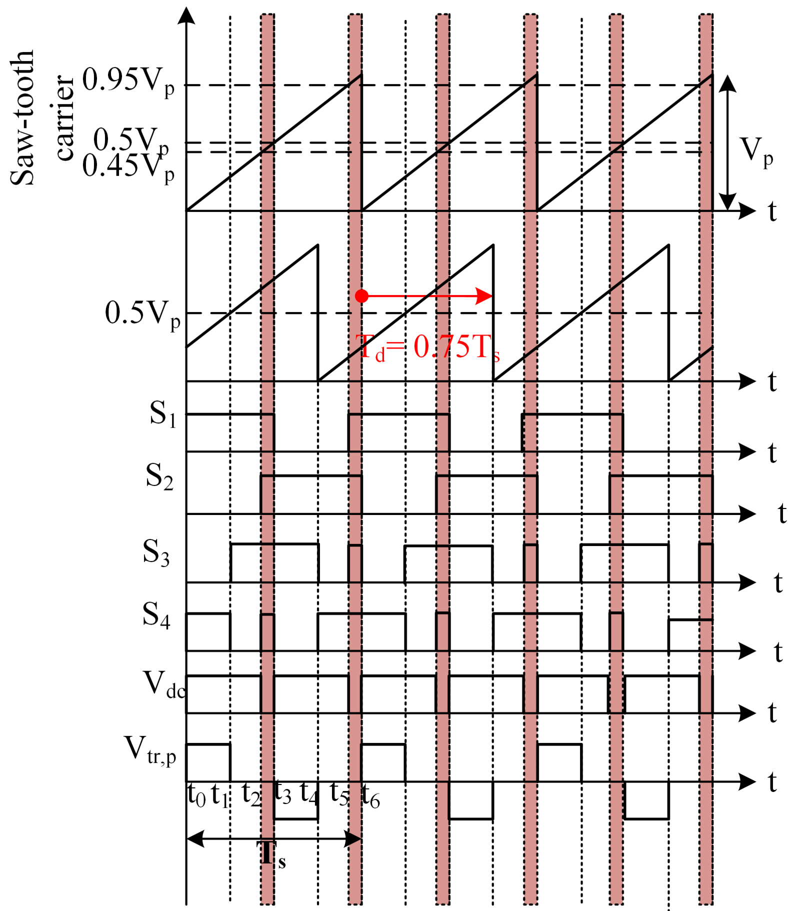

FIGURE 7 Switching waveforms of proposed topology in boost mode

3.2 | Reverse-power-flow control

During the reverse mode of operation, the converter works as a DAB converter with buck/boost functionality. The simplest control of a DAB is to provide a square-wave pulse to each H-bridge and control the phase shift between these bridges to regulate the amount and direction of power flow[21].

In this operation mode, the converter can operate with the phase-shift modulation technique. During this operation mode, each bridge is controlled with a 50% constant duty cycle generating a high-frequency square wave voltage at the transformer

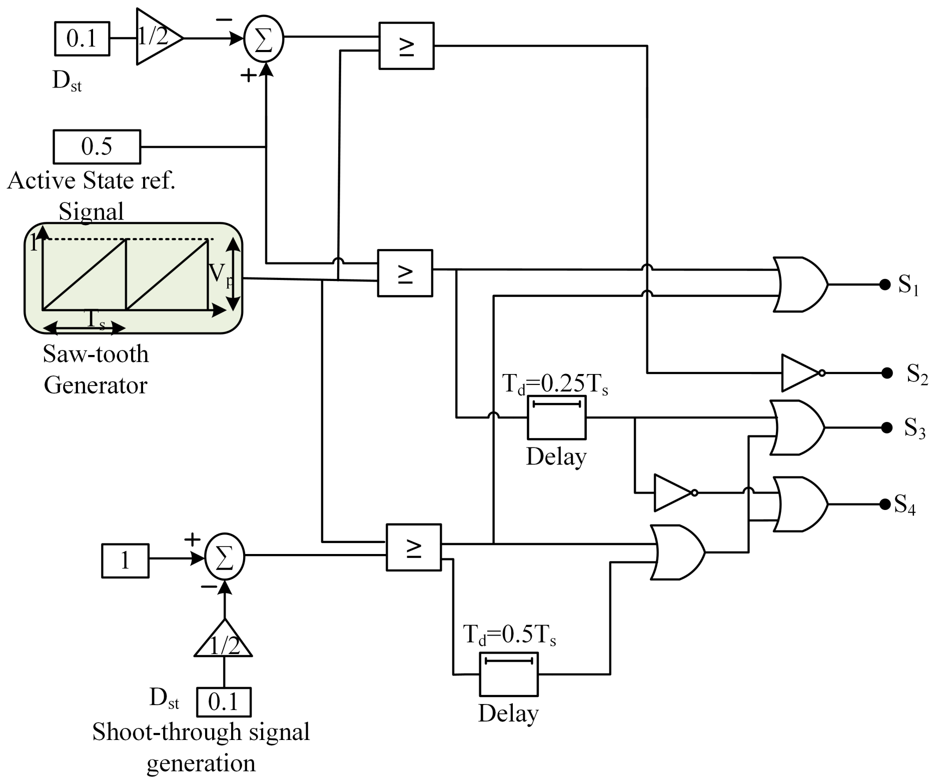

FIGURE 8 Gating Signal generation logic

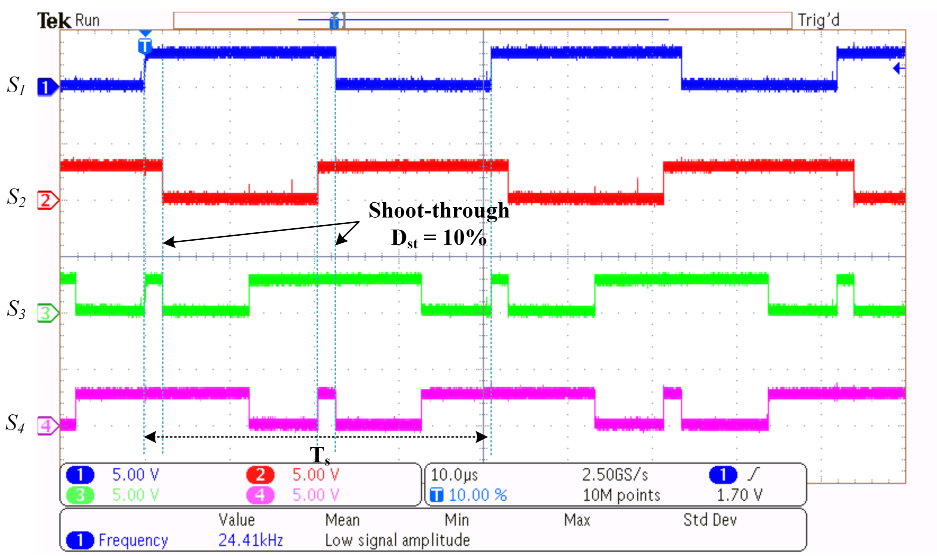

FIGURE 9 Gate pulse in forward-power-transfer mode with $D_{st} = 0.1$

terminals. The power-flow direction and amount are controlled by the phase shift between the two bridges. The power is delivered from right to left bridge, where the right bridge has a leading phase angle. The output power equation in this operation mode is given as:

$$P_O = \frac{V_1 V_2 n}{2\pi f_s L}\delta\left(1 - \frac{|\delta|}{\pi}\right) \tag{12}$$

where, f_s is the switching frequency, L is the equivalent inductance of the transformer referred to the primary side and δ is the phase shift between the two bridges in radians. From (12), the power flow depends on the switching frequency, equivalent inductance, and phase shift. As the switching frequency f_s is inversely proportional to the inductance, their product is constant. Thus, phase-shift ratio is a key parameter that limits the power flow. From (12), the maximum value of power flow occurs when the phase-shift angle is $\frac{\pi}{2}$. However, increasing δ will increase the reactive power, and typical phase shift values are in the range of 2- 15[16]. When δ is positive, the power flows from right bridge to left bridge and when it is negative from left to right. Typical transformer voltage and current waveforms when power is flowing in reverse-power-transfer mode and when $V_{tx,2} < V_{tx,1}$ are shown in Fig. 10 and the gate pulses during this mode are shown in Fig. 11 . As shown in Fig. 10 , the instantaneous value of current I_{l1} and I_{l2} can be calculated as[1] .

$$I_{l1} = -\frac{(V_{tx,2} + V_{tx,1})\delta + (V_{tx,2} - V_{tx,1})(\pi - \delta)}{2\pi f_s L} \tag{13}$$

$$I_{l2} = \frac{(V_{tx,2} + V_{tx,1})\delta - (V_{tx,2} - V_{tx,1})(\pi - \delta)}{2\pi f_s L} \tag{14}$$

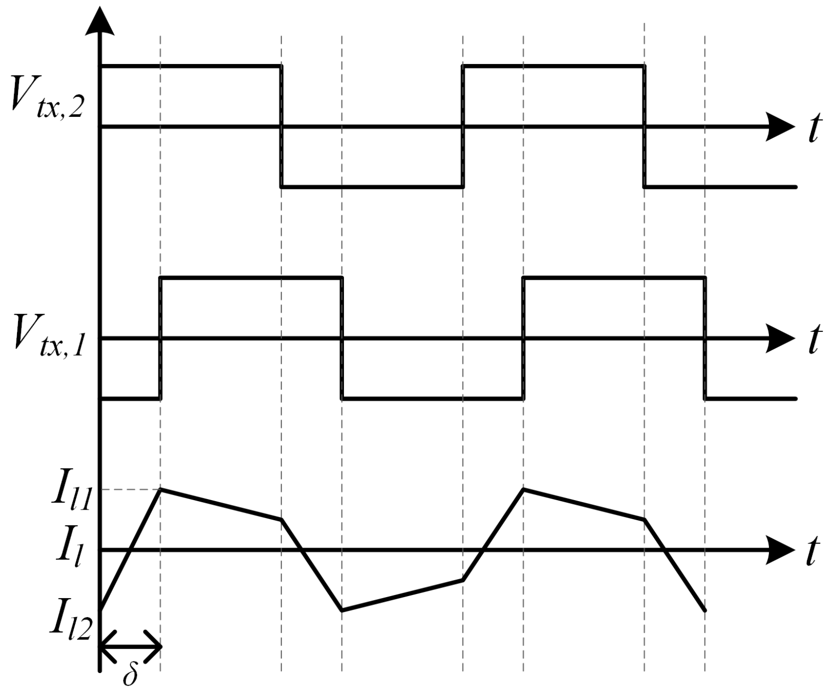

FIGURE 10 Operation waveforms of the converter in reverse-power-transfer mode

4 | COMPARISON WITH OTHER TOPOLOGIES

The performance of the proposed converter is compared with that of the existing DAB converter and impedance-source based isolated DC-DC converters from the literature[33]. Several factors have been considered for comparison with other topologies which includes number of active switches, range of soft switching, boosting ability, cost, reliability, input type, voltage regulation range, and control strategy. Table 1 shows the comparison of the proposed topology with others from the literature.

From Table 3 , it is clear that the proposed topology has superior advantages compared with existing ones from the literature. Some advantages of the proposed converter with respect other isolated bidirectional converter can be summarized as:

1. The proposed qDAB has higher boost ability and inherits all the other features of DAB. This is because of the insertion of a pre-boost impedance network stage which can boost the input voltage using the shoot-through duty cycle.

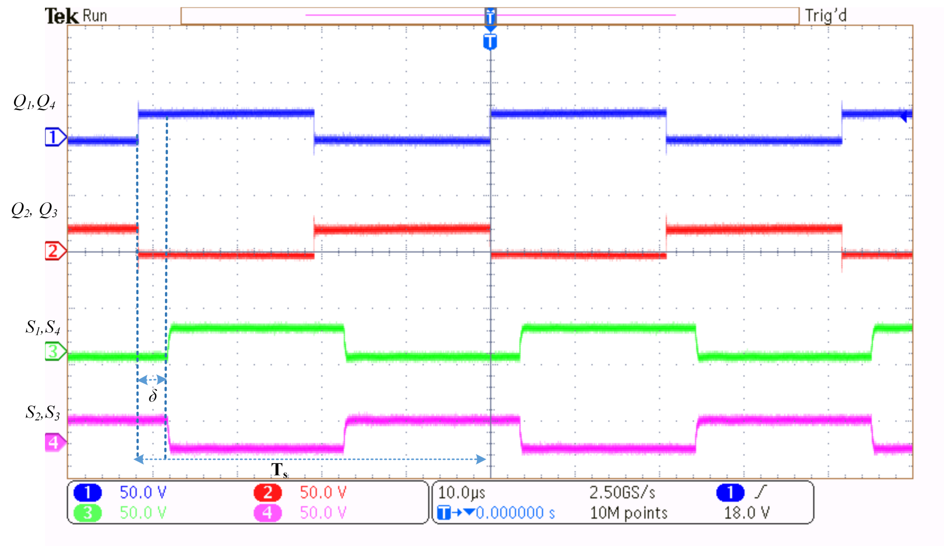

FIGURE 11 Gate pulses of the switches in reverse-power-transfer mode

TABLE 2 Summary of comparison for different isolated bidirectional converters

Parameters	DAB	[33]	[34]	Proposed
Active switch	8	12	6	9
Soft switching range	Narrow	None	Narrow	Wide
Boosting ability	Limited	High boost ratio	Limited	High boost ratio
Cost	Low	High	High	Medium
Reliability	Low	High	Low	High
Input source	Voltage	Voltage/current	Voltage	Voltage/current
Voltage regulation range	Low	High	Low	High
Control strategy	Simple	Complex	Complex	Simple

2. Reliability of the converter is also improved due to short-circuit immunity across the same leg.
3. The soft switching range is limited for DAB wherein the the modualtion scheme of the proposed converter provides ZVS on all switches irrespective of the load.
4. The control strategy of the proposed converter is simple as it only requires to control four switches during the forward power transfer mode while the body diode on the other side acts as a synchronous rectifier.
5. The output voltage of qDAB can be stepped up/down not only by the transformer turns ratio but also by the proposed modulation method, so it has wider voltage regulation range.
6. In addition to high boost ability, the proposed converter provides continuous input current and low voltage stress to the switch which is equal to output voltage.

5 | SIMULATION AND EXPERIMENTAL RESULTS

To verify the effectiveness of the proposed converter topology, a 500-W prototype was built and tested. A laboratory prototype shown in Fig. 12 is constructed based on TMS320F28335 DSP. The simulation was carried out using MATLAB Simulink software. The system parameters for both simulation and experiments are shown in Table 3 . The proposed bidirectional DC-DC converter was tested for both forward and reverse power-transfer operations. During forward-power-transfer mode, the converter

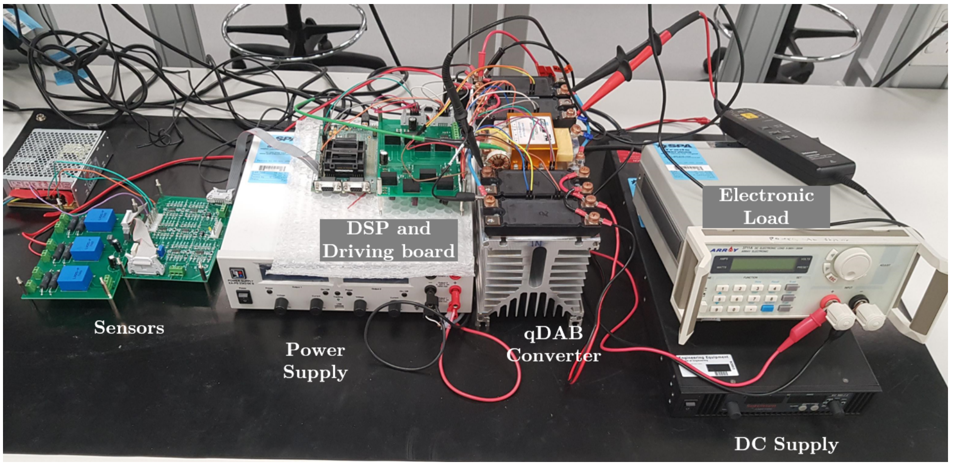

FIGURE 12 Photograph of the prototype

utilizes the shoot-through state, thereby performing the boost mode of operation while during the reverse-power-transfer mode the converter works as a buck/boost converter using the phase-shift modulation technique.

TABLE 3 Simulation/Experimental Parameters

Parameter	Value
Switching frequency	24 kHz
Switches (S_1-S_4 and Q_1-Q_4)	Sic MOSFET (BSM080D12P2C008)
Transformer Turns ratio	1:1
Inductors	1.7 mH
Capacitors	1000 μF
Input voltage, V_1	50 V
Power rating	500 W
Transformer leakage inductance	11.5 μH
Transformer winding resistance	20 $m\Omega$
Transformer magnetizing inductance	1.6 mH

5.1 | Boost mode in forward-power-transfer operation

For the boost mode of operation, 10% and 20% shoot-through states are added into the normal operational states of a qDAB. When the shoot-through duty cycle was set to be 10% the output voltage is boosted by the factor of B as indicated in (6) as shown in the simulation and experimental results in Fig. 13 and Fig. 14 . The input voltage, 50 V, was boosted to 62 V and the transformer voltage is symmetric, which avoids transformer saturation and reduces the output voltage ripple. The simulation and experimental results for the shoot-through duty cycle of 20 %, where the input voltage is boosted to 83 V is shown in Fig. 15 and Fig. 16 . The voltage spikes arise due to sudden transition in voltage level due to switching. These voltage spikes can be minimized using the larger electrolytic capacitor at the input side.

The soft switching on all switches are achieved with this proposed modulation technique. Unlike the DAB, where soft switching is limited to the rated load, this modulation method achieves soft switching in all legs for all load conditions. Figures 17 and 18 show the zero-voltage switching (ZVS) of switches S_1 and S_3. Similarly, switches S_2 and S_4 have the same switching pattern as S_1 and S_3. Thus, ZVS is achieved in all switches.

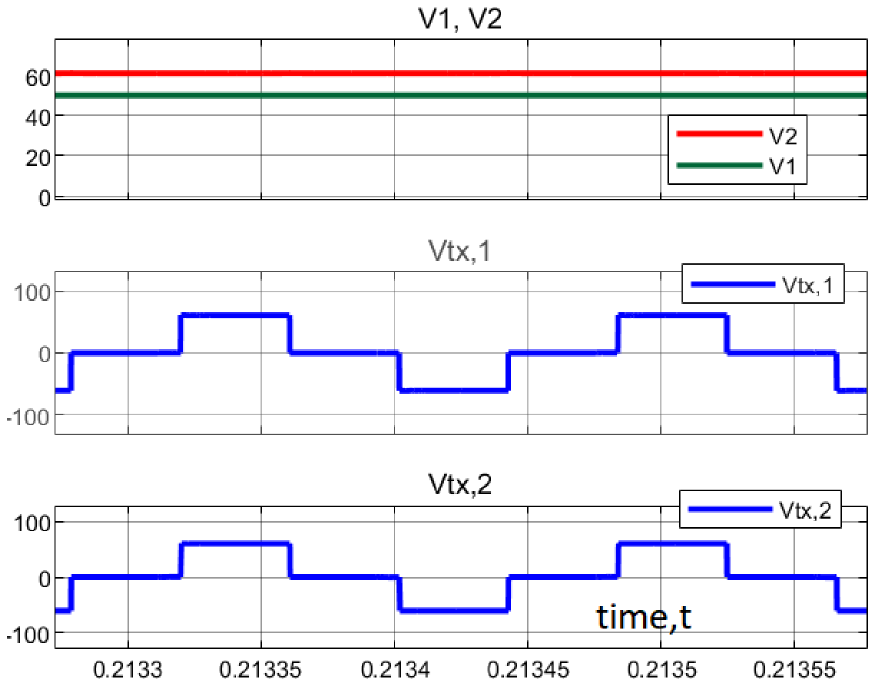

FIGURE 13 Simulation results: input/output voltage, transformer voltages for $D_{st} = 0.1$

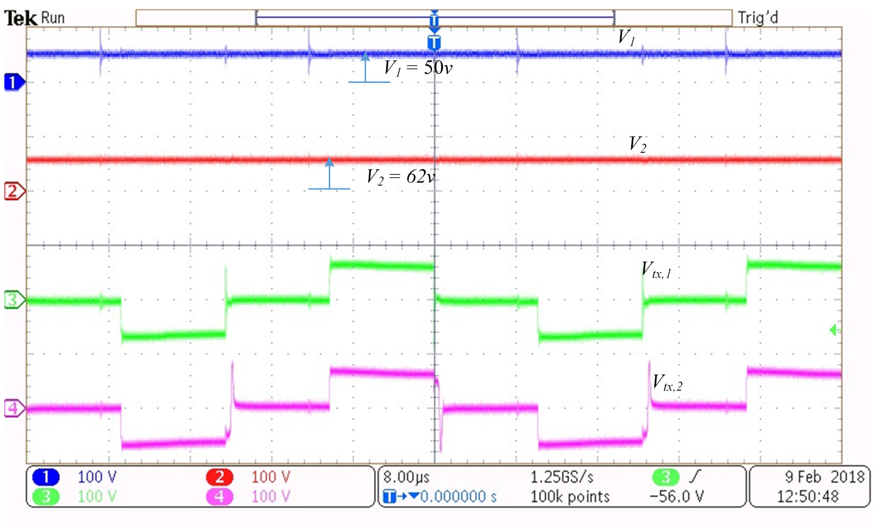

FIGURE 14 Experimental results: input/output voltage, transformer voltage. (Ch. 1: V_1 [100V/div]; Ch. 2: V_2 [100V/div]; Ch. 3: $V_{tx,1}$ [100V/div]; Ch. 4: $V_{tx,2}$ [100V/div] time: [8μs/div]).

5.2 | Buck/Boost operation in reverse-power-transfer mode

During the reverse-power-transfer mode, the converter works with the phase-shift modulation to transfer the power. Figure 19 shows the experimental results of the transformer voltages and current during this operational mode. The square-wave voltage of the secondary leads the primary voltage so that the power flows from the secondary bridge to the primary as indicated in (12). Figure 20 shows the observed waveform when the input voltage is 50 V, while the output is 57 V when the power is transferred from bridge 2 to bridge 1 with the phase-shift angle $\delta = 20^o$. The output voltage can be varied with a change of phase-shift angle, thus the converter has a flexibility of working as a buck/boost mode of operation using closed-loop operation.

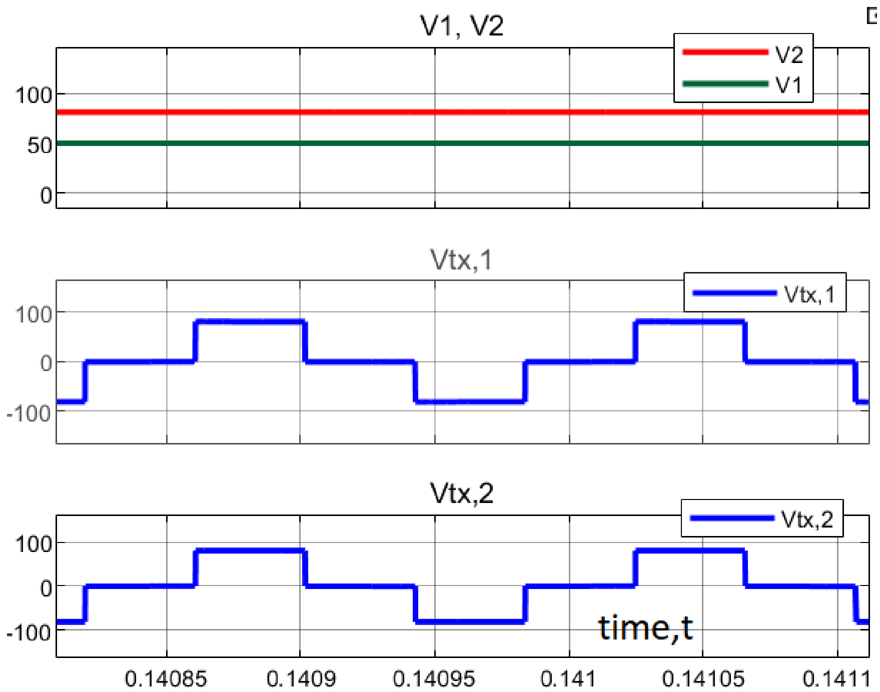

FIGURE 15 Simulation results: input/output voltage, transformer voltages for $D_{st} = 0.2$

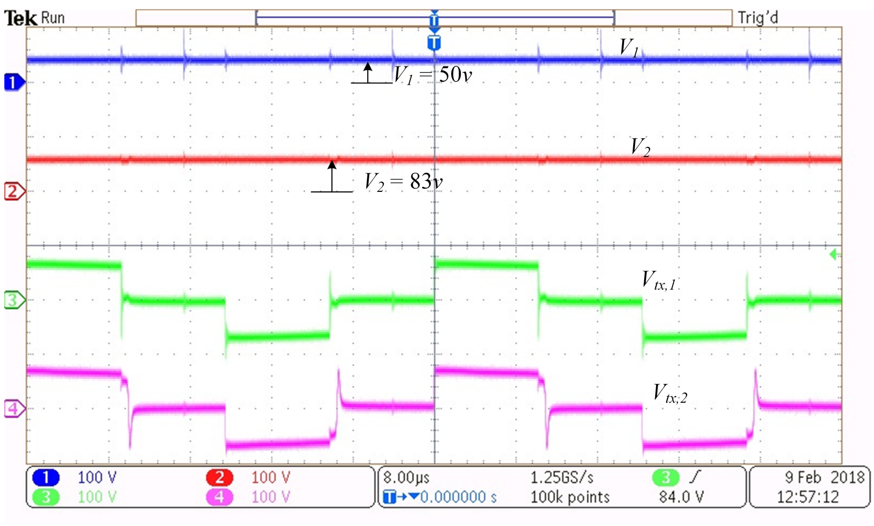

FIGURE 16 Experimental results: input/output voltage, transformer voltage. (Ch. 1: V_1 [100V/div]; Ch. 2: V_2 [100V/div]; Ch. 3: $V_{tx,1}$ [100V/div]; Ch. 4: $V_{tx,2}$ [100V/div] time: [8μs/div]).

Figure 21 shows how efficiency of the proposed converter varied with the load during forward power transfer mode.The peak efficiency was observed at 97% at zero-shoot through state when the converter was operated at the rated load of 500 W. The power loss in qDAB is mainly associated with switching, conduction loss and core losses across the magnetic components. A detail overview and mathematical investigation of these losses are presented in [35]

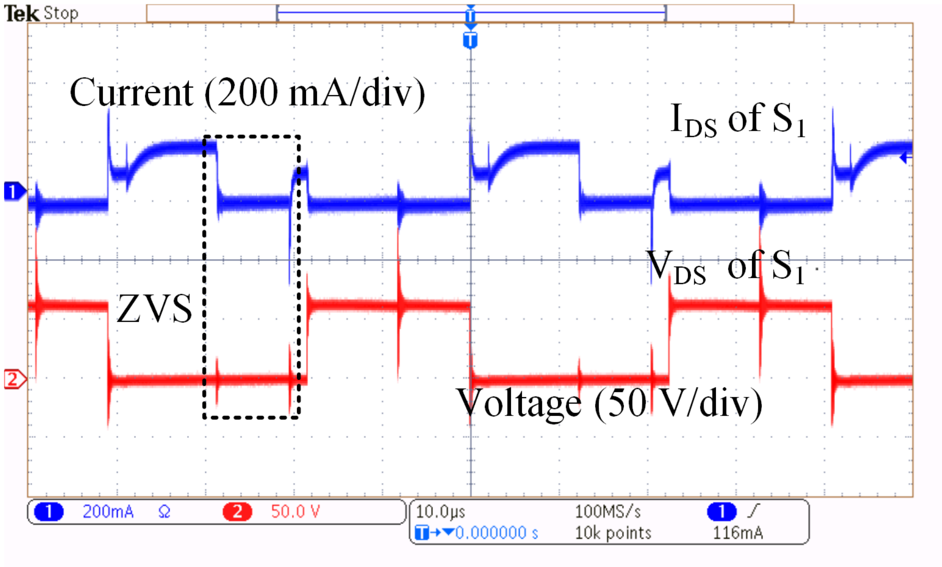

FIGURE 17 Drain-to-source voltage and current of S_1

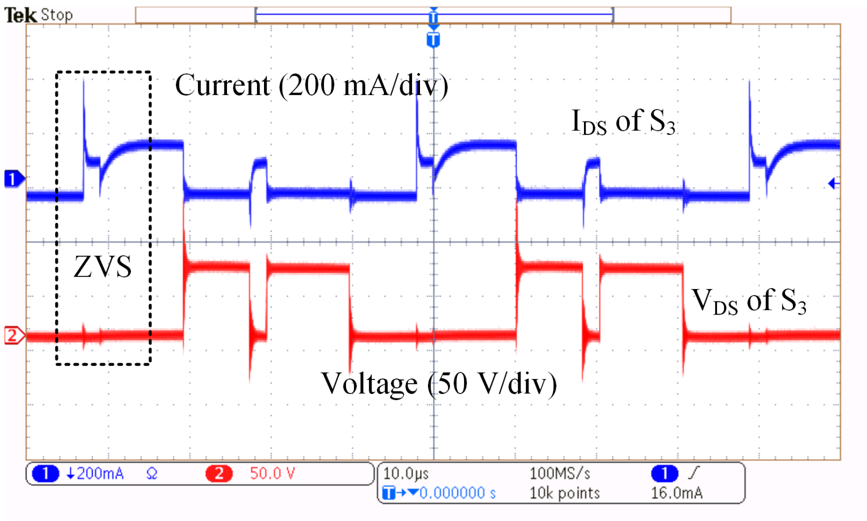

FIGURE 18 Drain-to-source voltage and current of S_3

6 | CONCLUSION

This paper proposes a quasi-Z-source based isolated bidirectional DC-DC converter applicable for renewable-energy systems. An impedance network is used to improve the boost ability of the conventional DAB converter. The converter works as a boost converter in the forward-power-transfer mode and buck/boost in the reverse mode of operation. It has a higher boost ability than the conventional DAB converter and inherits all the other features. The boost ability can be acquired not only by the transformer but also by the impedance-source network, so the converter's boost ability gets improved. Also, due to the immunity to short-circuits across the legs of the inverter, the reliability of the converter can be improved. Simulation and experimental results demonstrated the suitability of proposed topology and control method.

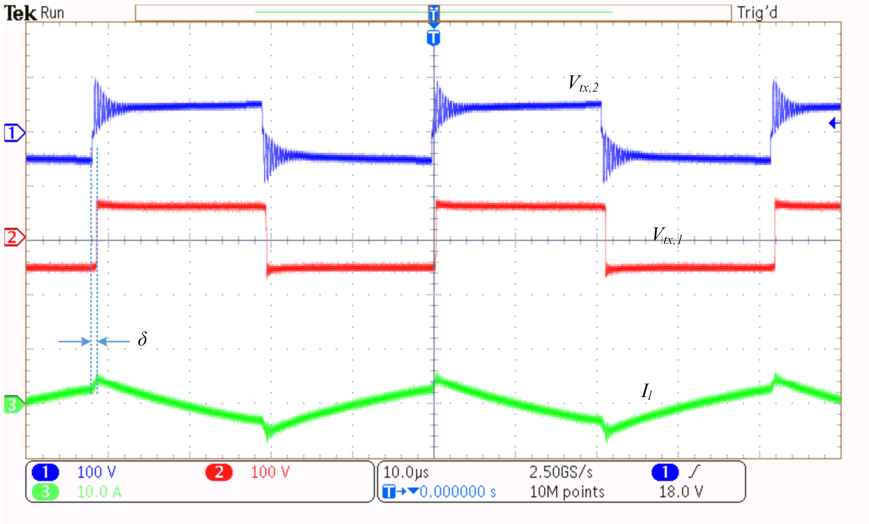

FIGURE 19 Experimental waveform of transformer voltage, transformer current in reverse-power-transfer mode when $\delta = 20^o$ (Ch. 1: $V_{tx,2}$ [100V/div]; Ch. 2: $V_{tx,1}$ [100V/div]; Ch. 3: I_L [10A/div];time: [10μs/div]).

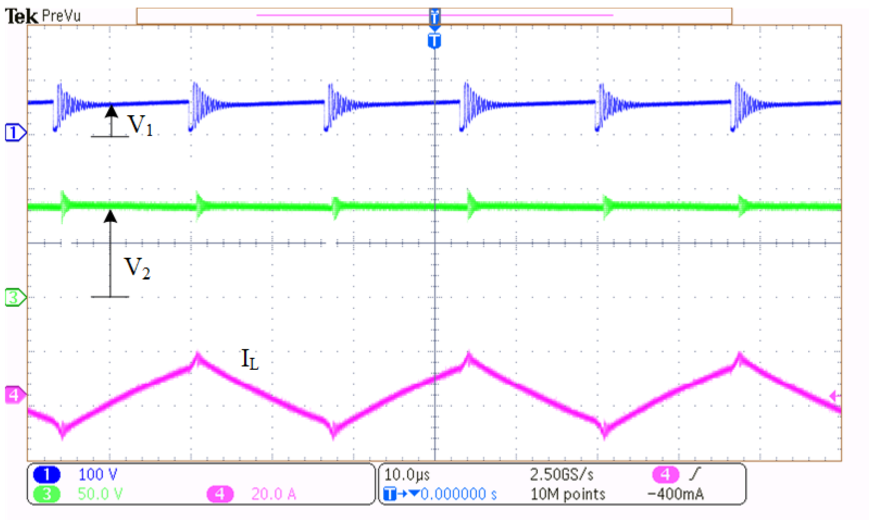

FIGURE 20 Experimental waveform of Input/output voltage and transformer current when $\delta = 20^o$ (Ch. 1: V_1 [100V/div]; Ch. 3: V_2 [50V/div]; Ch. 4: I_L [20A/div];time: [10μs/div]).

References

1. Inoue S, Akagi H. A bidirectional DC–DC converter for an energy storage system with galvanic isolation. *IEEE Transactions on Power Electronics* 2007; 22(6): 2299–2306.

2. Jain M, Daniele M, Jain PK. A bidirectional DC-DC converter topology for low power application. *IEEE Transactions on Power Electronics* 2000; 15(4): 595–606.

3. Mirzaei A, Jusoh A, Salam Z, Adib E, Farzanehfard H. Analysis and design of a high efficiency bidirectional DC–DC converter for battery and ultracapacitor applications. *Simulation Modelling Practice and Theory* 2011; 19(7): 1651–1667.

4. Blinov A, Kosenko R, Chub A, Vinnikov D. Bidirectional soft-switching dc-dc converter for battery energy storage systems. *IET Power Electronics* 2018; 11(12): 2000-2009. doi: 10.1049/iet-pel.2018.5054

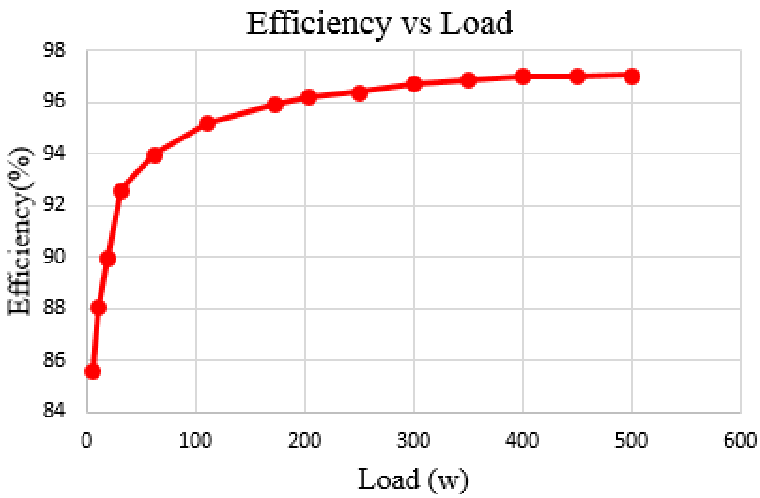

FIGURE 21 Efficiency of the converter at different load.

5. He P, Khaligh A. Comprehensive analyses and comparison of 1 kW isolated DC–DC converters for bidirectional EV charging systems. *IEEE Transactions on Transportation Electrification* 2017; 3(1): 147–156.

6. Zhang Y, Liu Q, Li J, Sumner M. A Common Ground Switched-Quasi-Z -Source Bidirectional DC–DC Converter With Wide-Voltage-Gain Range for EVs With Hybrid Energy Sources. *IEEE Transactions on Industrial Electronics* 2018; 65(6): 5188-5200.

7. Na T, Zhang Q, Dong S, Raherimihaja HJ, Chuai G, Wang J. A Soft-Switched Modulation for a Single-Phase Quasi-Z-Source-Integrated Charger in Electric Vehicle Application. *IEEE Transactions on Power Electronics* 2020; 35(5): 4602-4612.

8. Chiu HJ, Lin LW. A bidirectional DC–DC converter for fuel cell electric vehicle driving system. *IEEE Transactions on Power Electronics* 2006; 21(4): 950–958.

9. Torrico-Bascopé RP, OliveiraJr DS, Branco CG, Antunes FL. A UPS with 110-V/220-V input voltage and high-frequency transformer isolation. *IEEE Transactions on Industrial Electronics* 2008; 55(8): 2984–2996.

10. Tao H, Duarte JL, Hendrix MAM. Line-Interactive UPS Using a Fuel Cell as the Primary Source. *IEEE Transactions on Industrial Electronics* 2008; 55(8): 3012-3021. doi: 10.1109/TIE.2008.918472

11. Qin H. Dual active bridge converters in solid state transformers. 2012.

12. Tofoli FL, Castro Pereira dD, Paula dWJ, Júnior DdSO. Survey on non-isolated high-voltage step-up dc–dc topologies based on the boost converter. *IET power Electronics* 2015; 8(10): 2044–2057.

13. Duan R, Lee J. High-efficiency bidirectional DC-DC converter with coupled inductor. *IET Power Electronics* 2012; 5(1): 115-123. doi: 10.1049/iet-pel.2010.0401

14. Ardi H, Reza Ahrabi R, Najafi Ravadanegh S. Non-isolated bidirectional DC-DC converter analysis and implementation. *IET Power Electronics* 2014; 7(12): 3033-3044. doi: 10.1049/iet-pel.2013.0898

15. Zhang C, Gao Z, Liao X. Bidirectional DC-DC converter with series-connected resonant tanks to realise soft switching. *IET Power Electronics* 2018; 11(12): 2029-2043. doi: 10.1049/iet-pel.2018.5311

16. De Doncker RW, Divan DM, Kheraluwala MH. A three-phase soft-switched high-power-density DC/DC converter for high-power applications. *IEEE transactions on industry applications* 1991; 27(1): 63–73.

17. Krismer F, Kolar JW. Accurate Power Loss Model Derivation of a High-Current Dual Active Bridge Converter for an Automotive Application. *IEEE Transactions on Industrial Electronics* 2010; 57(3): 881-891. doi: 10.1109/TIE.2009.2025284

18. Kheraluwala MN, Gascoigne RW, Divan DM, Baumann ED. Performance characterization of a high-power dual active bridge DC-to-DC converter. *IEEE Transactions on Industry Applications* 1992; 28(6): 1294-1301. doi: 10.1109/28.175280

19. Bai H, Mi C. Eliminate Reactive Power and Increase System Efficiency of Isolated Bidirectional Dual-Active-Bridge DC–DC Converters Using Novel Dual-Phase-Shift Control. *IEEE Transactions on Power Electronics* 2008; 23(6): 2905-2914. doi: 10.1109/TPEL.2008.2005103

20. Tao H, Kotsopoulos A, Duarte JL, Hendrix MAM. Transformer-Coupled Multiport ZVS Bidirectional DC-DC Converter With Wide Input Range. *IEEE Transactions on Power Electronics* 2008; 23(2): 771-781. doi: 10.1109/TPEL.2007.915129

21. Mi C, Bai H, Wang C, Gargies S. Operation, design and control of dual H-bridge-based isolated bidirectional DC–DC converter. *IET Power Electronics* 2008; 1(4): 507–517.

22. Peng FZ. Z-source inverter. *IEEE Transactions on industry applications* 2003; 39(2): 504–510.

23. Peng F. Z-source inverter. In: . 2. IEEE. ; 2002: 775–781.

24. Siwakoti YP, Peng FZ, Blaabjerg F, Loh PC, Town GE. Impedance-source networks for electric power conversion part I: A topological review. *IEEE Transactions on Power Electronics* 2015; 30(2): 699–716.

25. Alizadeh Pahlavani MR, Hasan Babayi Nozadian M. High step-up active Z-source dc/dc converters; analyses and control method. *IET Power Electronics* 2019; 12(4): 790-800. doi: 10.1049/iet-pel.2018.5554

26. Liu H, Li F, Wheeler P. A Family of DC-DC Converters Deduced From Impedance Source DC-DC Converters for High Step-Up Conversion. *IEEE Transactions on Industrial Electronics* 2016; 63(11): 6856-6866. doi: 10.1109/TIE.2016.2582826

27. Ortega M, Ortega MV, Jurado F, Carpio J, Vera D. Bidirectional DC-DC converter with high gain based on impedance source. *IET Power Electronics* 2019; 12(8): 2069-2078. doi: 10.1049/iet-pel.2018.5385

28. Vinnikov D, Roasto I. Quasi-Z-source-based isolated DC/DC converters for distributed power generation. *IEEE Transactions on Industrial Electronics* 2011; 58(1): 192–201.

29. Haji-Esmaeili MM, Babaei E, Sabahi M. High Step-Up Quasi-Z Source DC-DC Converter. *IEEE Transactions on Power Electronics* 2018; 33(12): 10563-10571. doi: 10.1109/TPEL.2018.2810884

30. Kafle YR, Hasan SU, Town GE. Quasi-Z-source based bidirectional DC-DC converter and its control strategy. *Chinese Journal of Electrical Engineering* 2019; 5(1): 1-9. doi: 10.23919/CJEE.2019.000001

31. Anderson J, Peng FZ. Four quasi-Z-source inverters. In: IEEE. ; 2008: 2743–2749.

32. Li Y, Anderson J, Peng FZ, Liu D. Quasi-Z-Source Inverter for Photovoltaic Power Generation Systems. In: ; 2009: 918-924

33. Zhao B, Yu Q, Leng Z, Chen X. Switched Z-Source Isolated Bidirectional DC- DC Converter and Its Phase-Shifting Shoot-Through Bivariate Coordinated Control Strategy. *IEEE Transactions on Industrial Electronics* 2012; 59(12): 4657-4670. doi: 10.1109/TIE.2011.2181136

34. Cao L, Loo KH, Lai YM. Output-Impedance Shaping of Bidirectional DAB DC–DC Converter Using Double-Proportional-Integral Feedback for Near-Ripple-Free DC Bus Voltage Regulation in Renewable Energy Systems. *IEEE Transactions on Power Electronics* 2016; 31(3): 2187-2199.

35. Pittini R, Zhang Z, Andersen MAE. Isolated full bridge boost DC-DC converter designed for bidirectional operation of fuel cells/electrolyzer cells in grid-tie applications. In: ; 2013: 1-10

How to cite this article: Y. Kafle, M.J. Hossain, and M. Kashif (2020), Impedance-Source-based Bidirectional DC-DC Converters for Renewable Energy Applications, *Int Trans Electr Energ Syst*, *2020;00:1–6*.